nature geoscience
SUPPLEMENTARY INFORMATION
DOI: 10.1038/NGEO2375

Dynamics of the intertropical convergence zone over the western Pacific during the Little Ice Age

Hong Yan, Wei Wei, Willie Soon, Zhisheng An, Weijian Zhou, Zhonghui Liu, Yuhong Wang, Robert M. Carter

This file includes:

Supplementary discussion

Supplementary Figure s1 to s10

Supplementary Table s1

References

Supplementary discussion:

Supporting evidence from decadal-multidecadal-centennial scale oscillations

In addition to the MCA-LIA-recent 150 years transition, other multidecadal-scale oscillations in solar output have also occurred over the last millennium[1,2]. If solar output is a significant factor for tropical hydrologic variation over the last millennium, then the paleo-hydrology records should have recorded the signals of these oscillations. Although most proxy-hydrology records are low resolution, and not accurately dated enough to capture decadal-centennial-scale variations, such oscillations have been detected in several high resolution precipitation records from the Asian-Australian monsoon area. These multi-decadal hydrologic variations are consistent with our proposal of a contracted monsoon/ITCZ during solar irradiance minimum. For example, some decadal changes in a speleothem record from north China[3] and a coral record from northeast Australia[4] are correlated with decadal variations of the solar irradiance, with increased rainfall during the peaks of the solar activity (D4 and D8 records in Fig. s10). Meanwhile, and conversely, hydrological records from the western Pacific region[5] reveal increased rainfall during the troughs of the solar output (W2 record in Fig. s10). An increased rainfall in the tropical western Pacific during the solar minimum was also supported by a recent study which found that the precipitation in Indonesia increased abruptly at the time of the solar minimum around 2800 yr BP[6].

On the other hand, power spectrum analysis indicates that the periodicities of the speleothem $\delta^{18}O$ series from monsoonal China[3,7-9] are similar to and consistent with the presence of solar cycles - such as the well known 80-120 yr and ~20 yr periodicities.

It is important to note, however, that not all the variations in rainfall records from the Asian-Australian monsoon area exhibit good correspondence with solar output. For example, no multi-decadal oscillations were observed in fluvial sedimentary records from the Magela Creek Flood Plain[10]. However, good reasons exist that could explain disagreements between decadal variation in a proxy record and the solar activity record. Those reasons include time delays for hydrologic changes in response to solar activity forcing, spatial differences of the local and regional rainfalls in response to the solar forcing (e.g., wet, dry and no changes in different regions in response to the same solar minima) and a lack of quality in particular proxy records (e.g. time resolution, error of age model).

Finally, it is noteworthy that the impacts of decadal to centennial scale cycles in solar activity on tropical hydrology have long been known to occur in speleothem, lake and marine sediment records from tropical Latin America, central Africa and elsewhere[11-17].

The contraction of ITCZ and the strengthening of Pacific Walker Circulation during LIA

The extended clear dry conditions that obtained in mid-northern part of the mainland China and northern Australia during the LIA are consistent with the disappearance or weakening of the ITCZ/monsoonal rainfall in these regions, and point to a contraction of the ITCZ’s sphere of influence (see the summary presented in Fig. s6 and s7). At the same time, the precipitation zones converged more narrowly within the tropics and resulted in more rainfall in the Indo-Pacific warm-fresh pool region. However, the contracted ITCZ/monsoon was probably not the only cause of dilution of the warm pool. As well, concurrent changes of ENSO/Walker circulation, which today has a big impact on modern western Pacific hydrology, probably contributed to the changes in multi-decadal to centennial- scale precipitation in this region[5,18,19].

Indeed, a number of papers have addressed the ENSO/Walker circulation variations in the tropical Pacific during the past millennium. Overall, the results remain unclear, controversy stemming from a perceived contradiction between the reduced east-west tropical Pacific SST gradient (El Niño-like) and the enhanced Pacific Walker circulation (La Niña-like)[20]. The best available SST reconstructions in the western[19,21], eastern[22,23] and mid[24] tropical Pacific suggest[25,26] an LIA marked by relative warming in the eastern and central tropical Pacific, accompanied by substantial cooling in the western equatorial ocean and a more El Niño-like state (when compared and contrasted with conditions during the MCA). In contrast, nearly all hydrological reconstructions from the tropical Pacific suggested a more La Niña-like mean state during the LIA than during the MCA. These include records from the Indo-Pacific[5,18,19,21,27], the central tropical Pacific [28] and the eastern equatorial Pacific[29,30] that indicate wetter, drier and drier conditions, respectively, during the LIA than during the MCA. Meanwhile, theoretical models and computer simulations also project contradictory results for the mean climatic state during the LIA and the MCA. For example, the "ocean dynamical thermostat" mechanism[31-33] predicts a more El Niño-like state in the LIA than in the MCA, while the coupled general circulation models (CGCM) project a possible strengthening of the Walker circulation (La Niña-like state) during the LIA[34,35] (see ref[20] for detailed discussion). Several co-working factors could contribute to explain the conflict between the SST records and the hydrological records, such as the inappropriate interpretation of the current SST/hydrological records (e.g. the primary mode of the SST or hydrological records in tropical Pacific on centennial scale perhaps might not be ENSO variation, but instead represent the meridional temperature gradient or ITCZ changes). A decoupling between the atmospheric and oceanic response to forcing on centennial timescales is another possibility. More high-resolution proxy records and climate models are thus needed in the future research that seeks to clarify this unresolved puzzle.

In summary, although the temperature-based reconstructions indicate an El Nino-like SST pattern existed in the tropical Pacific during the LIA[24,25], the hydrological studies, based upon either proxy records[5,18,19,29] or model simulations[34], present a clear strengthening of the Pacific Walker circulation during the LIA, which in turn would cause increased precipitation in the Indo-Pacific warm-fresh pool region. Moreover, the model results in this study also implied an increased zonal precipitation contrast between east and west tropical Pacific during the LIA (Fig. s9 and ref[36]), which would probably also manifest itself as an enhanced Pacific Walker circulation. That is to say, the contracted western Pacific monsoon/ITCZ and enhanced Pacific Walker circulation probably co-existed during the LIA interval, with both mechanisms contributing extra precipitation to the wet and warm pool region of the western Pacific.

This co-existence of a contracted ITCZ/monsoon and strengthened Pacific Walker circulation during the LIA raises some issues that need to be addressed in future studies. For example, both ITCZ contraction and Walker circulation strengthening could increase convection in the western Pacific warm pool, but which factor is the dominant cause? Also, what interaction, if any, occurs between ITCZ behavior and Walker circulation on multi-decadal to centennial scales (e.g., the contraction of the western Pacific marine-continental ITCZ could increase convection activity in the western Pacific, and therefore enhance Pacific Walker Circulation)?

A brief description of the ECHO-G and MPI-ESM models: Ability to simulate global monsoon and monsoon-related climate variations

ECHO-G model: the ECHO-G model has very reasonable performance on simulating the monsoonal precipitation. In Liu et al. (2009)[36], the authors have compared the simulated annual mean precipitation and global monsoon mode with those from the observation and reanalysis data (Figure 1 in their paper). They show quite consistent patterns and confirm the reliability of the model performance. In this paper, the authors have conducted two ECHO-G experiments, one with fixed external forcing used as a control experiment and the other with three external forcings, i.e. solar variability, greenhouse gas concentration and volcanic forcing[36].

MPI-ESM model: the basic model simulation and capability of MPI-ESM for the last millennium has been described by Jungclaus et al. (2010)[37]. Although there is no special focus on the performance of the model on monsoonal precipitation in that paper, a follow-up paper by Man et al. (2012)[38] studied theEast Asian summer monsoon during the last millennium. Man et al. (2012) compared the simulated summer precipitation over the East Asian monsoon region with that observed, using reanalysis data. Figure 2 in their paper reports good agreement among datasets regarding the precipitation and the 850-hpa wind patterns. After the validation of the simulation results, the authors also demonstrated that the model can capture the East Asian summer monsoon change during the MCA and LIA periods via model-data comparison. Hence, the works by Man et al. (2012) add confidence to our use of MPI-ESM model for studying the TSI-induced ITCZ contraction hypothesis around the Indo-Pacific warm-fresh pool region during the Little Ice Age interval.

Supplementary Figures

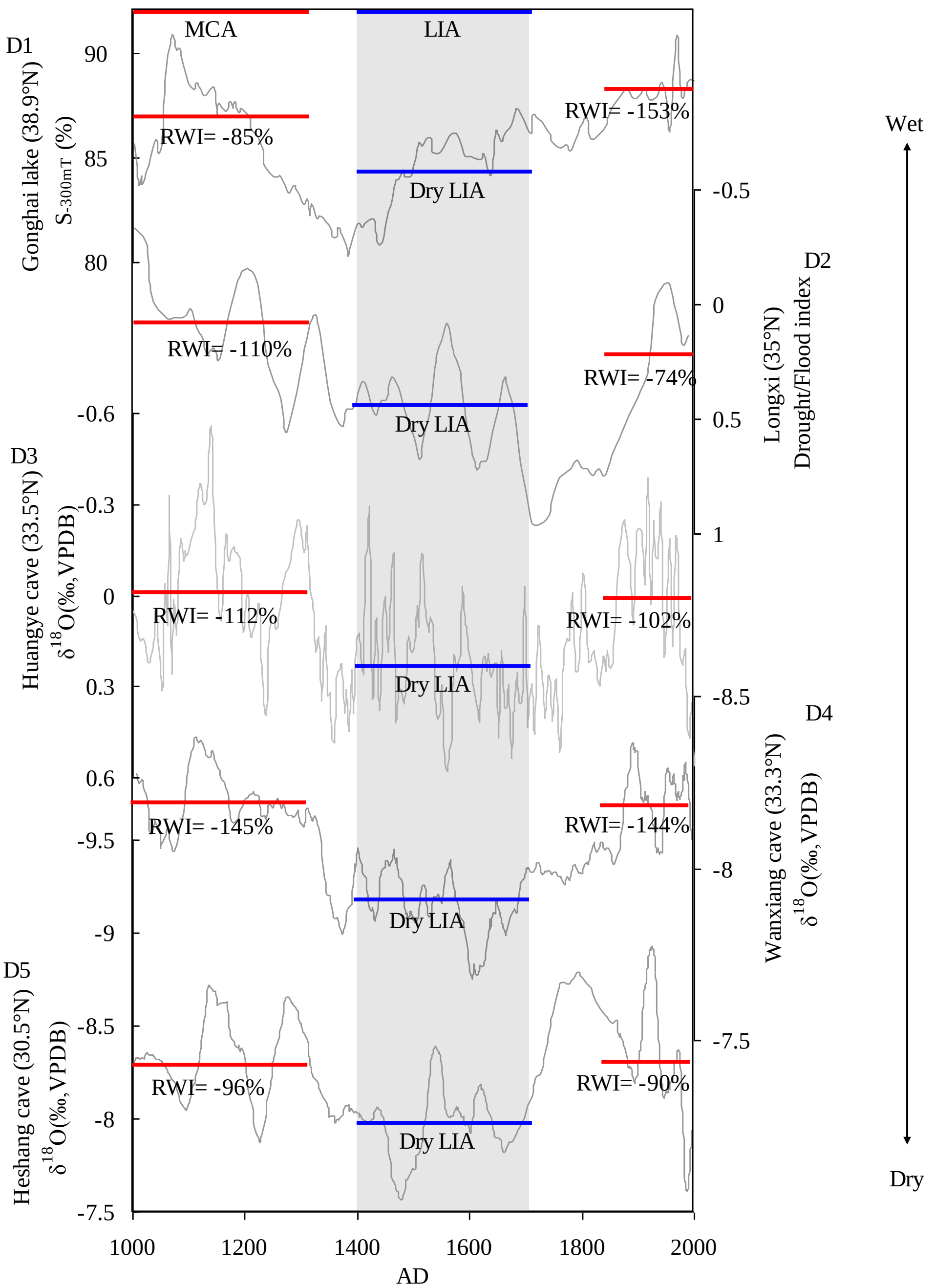

Figure s1: Hydrologic proxy records D1[39], D2[40], D3[8], D4[3] and D5[7] from the EASM area showing dry condition during the LIA relative to MCA/recent 150 years. The locations of these records are shown in Fig.1. Please see the Methods section for the definitions of the Relative Wet Index (RWI) and the wet/dry condition during the LIA relative to the MCA/recent 150 years.

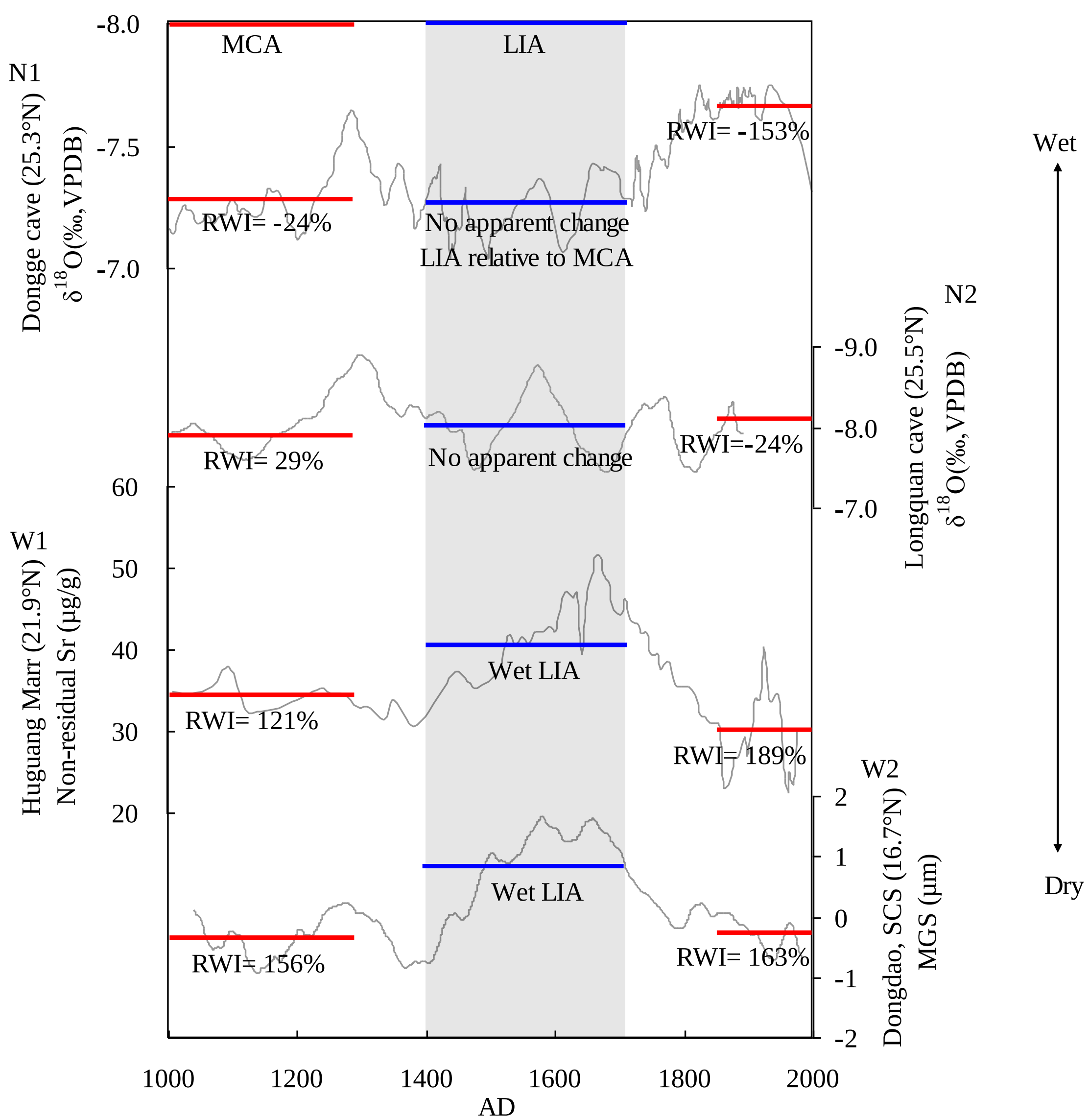

Figure s2: Hydrologic proxy records N1[9], N2[41], W1[42,43] and W2[5,27] from the EASM area indicate no apparent change of rainfall and wet conditions during the LIA relative to the MCA. The locations of these records are shown in Fig.1. Please see the Methods section for the definitions of the Relative Wet Index (RWI) and the wet/dry condition during the LIA relative to the MCA/recent 150 years.

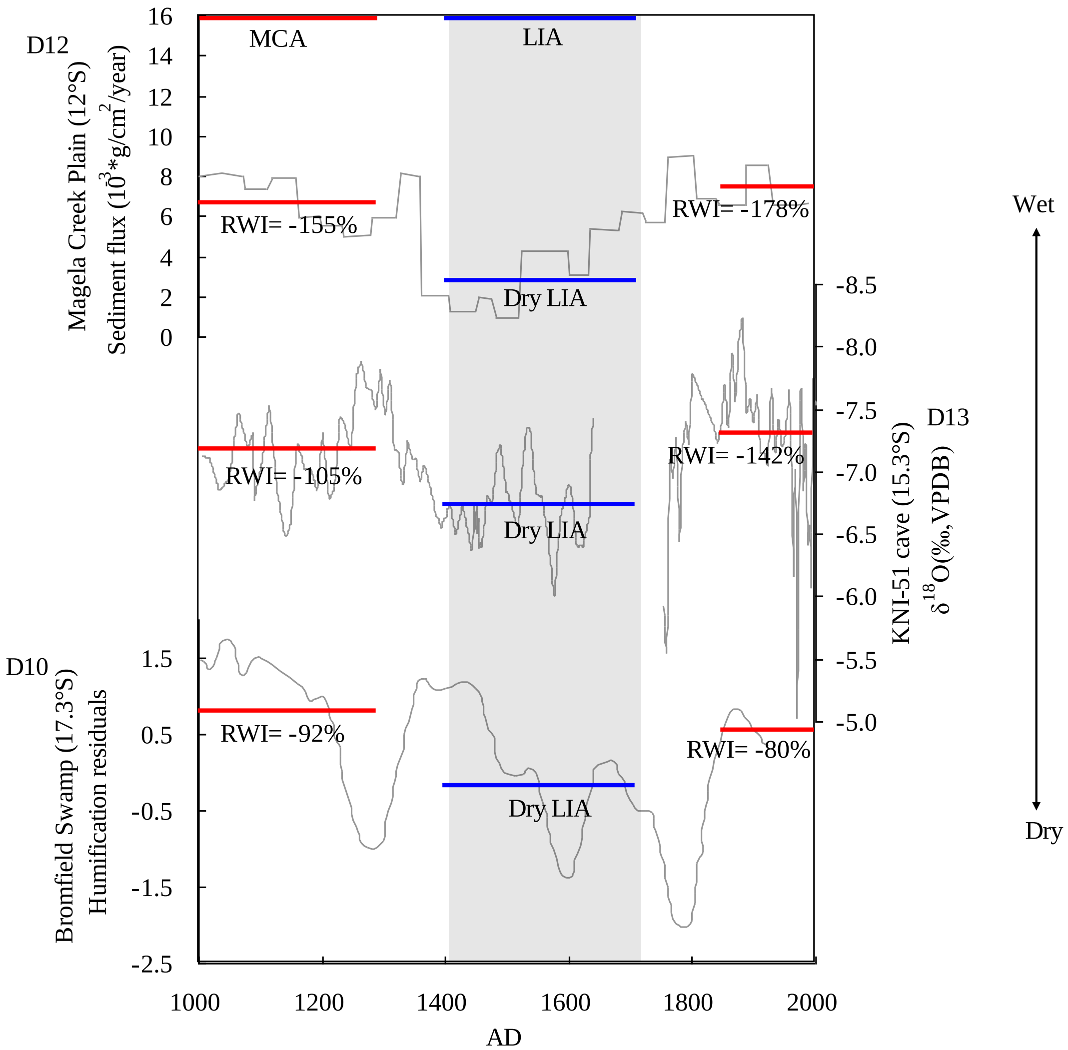

Figure s3: Hydrologic proxy records D10[44,45], D12[10], D13[46] from the northern Australia monsoon area showing dry condition during the LIA relative to the MCA/recent 150 years. The locations of these records are shown in Fig. 2. Please see the Method section for the definitions of the Relative Wet Index (RWI) and the wet/dry condition during the LIA relative to the MCA/recent 150 years.

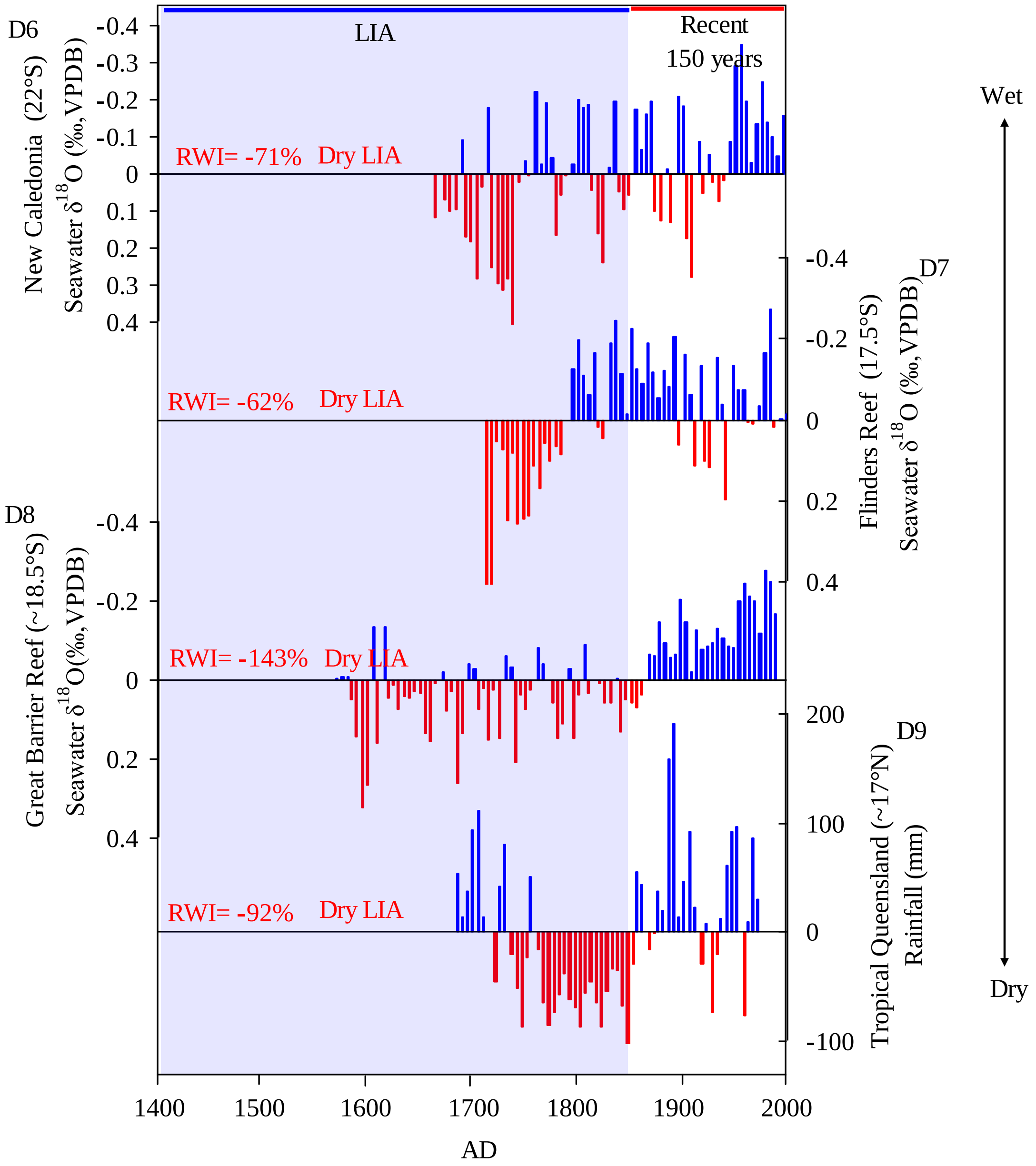

Figure s4: Coral records D6[47-49], D7[50], D8[4] and D9[51] from northeast Australia showing dry conditions during the LIA relative to the last 150 years (i.e., D6, D7 and D8: seawater $\delta^{18}O$ record calculated from the coral $\delta^{18}O$ and Sr/Ca; D9: rainfall reconstruction in Great Barrier Reef derived from coral luminescence). The locations of these records are shown in Fig. 2. Please see the Methods section for the definitions of the Relative Wet Index (RWI) and the wet/dry condition during the LIA relative to the most recent 150 years.

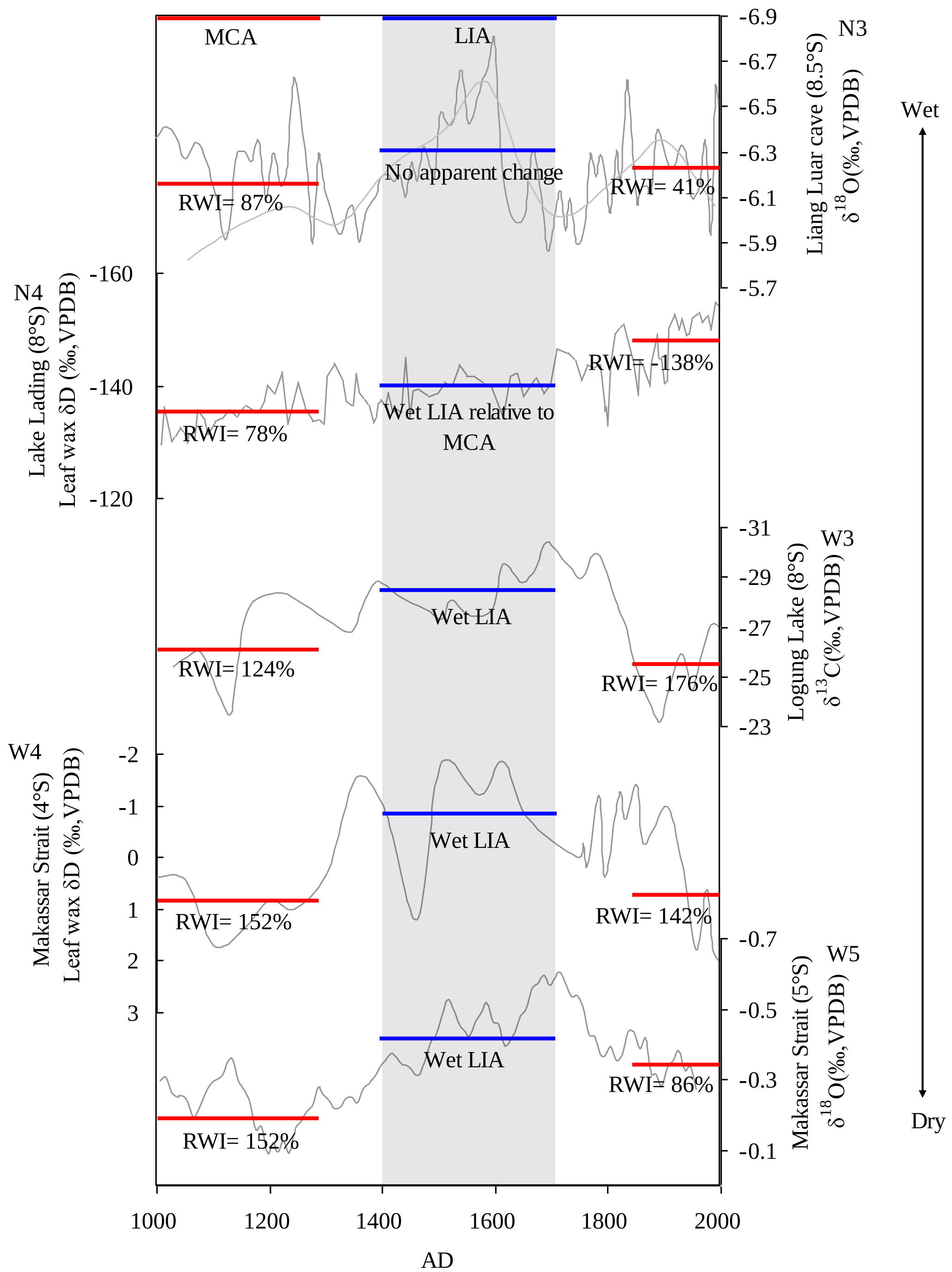

Figure s5: Proxy hydrology records N3[52], N4[53], W3[54], W4[18] and W5[19,21] from the ASM area indicate no apparent change of rainfall and wet conditions during the LIA relative to the MCA. The locations of these records are shown in Fig. 2. Please see the Method section for the definitions of the Relative Wet Index (RWI) and the wet/dry condition during the LIA relative to the MCA/recent 150 years.

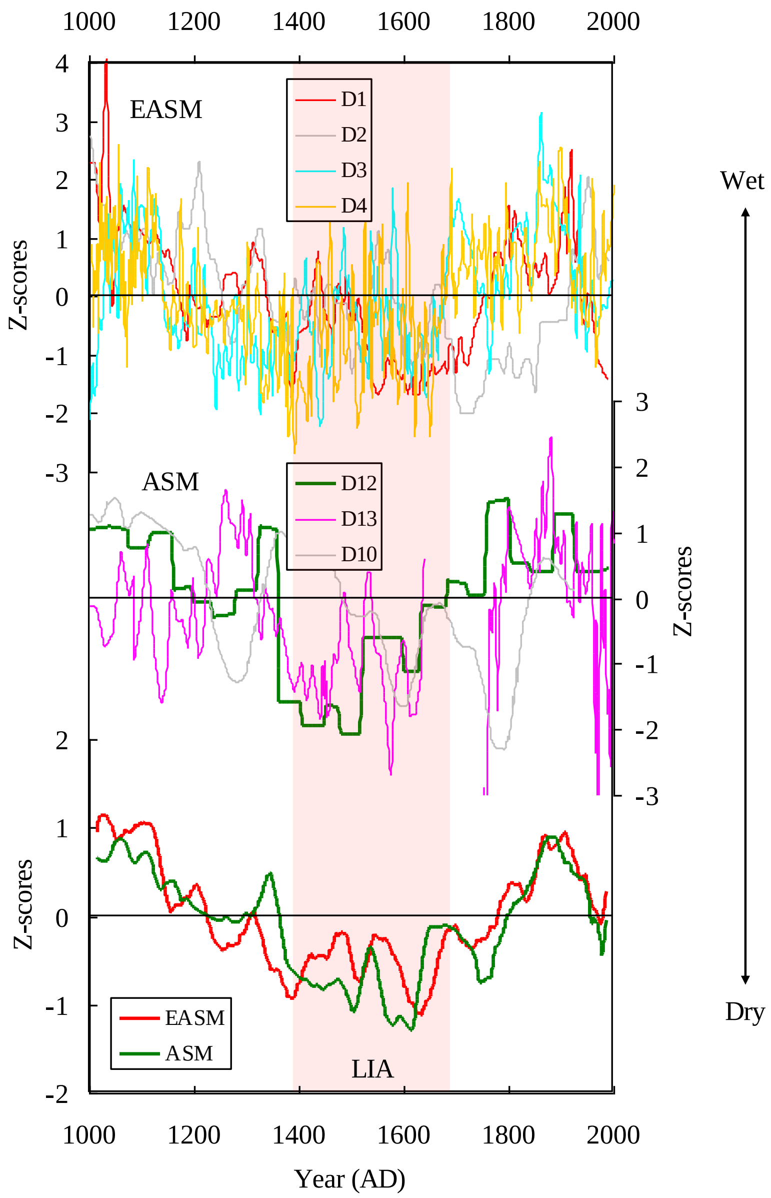

Figure s6: Near synchronous retreat of the EASM and the ASM during the LIA. Hydrological records from the front areas of the EASM (top panel) and the ASM (middle panel). The composite hydrological changes (30 years smoothing) of the EASM (the average of records D1, D2, D3 and D4) and the ASM (the average of records D10, D12 and D13) are shown in the bottom panel. All proxy records are normalized to standard Z-scores. Standard Z-scores are calculated according to Z=(X-V)/SD; where X is original value, V is the averaged of each time series, and SD is the standard deviation of each time series.

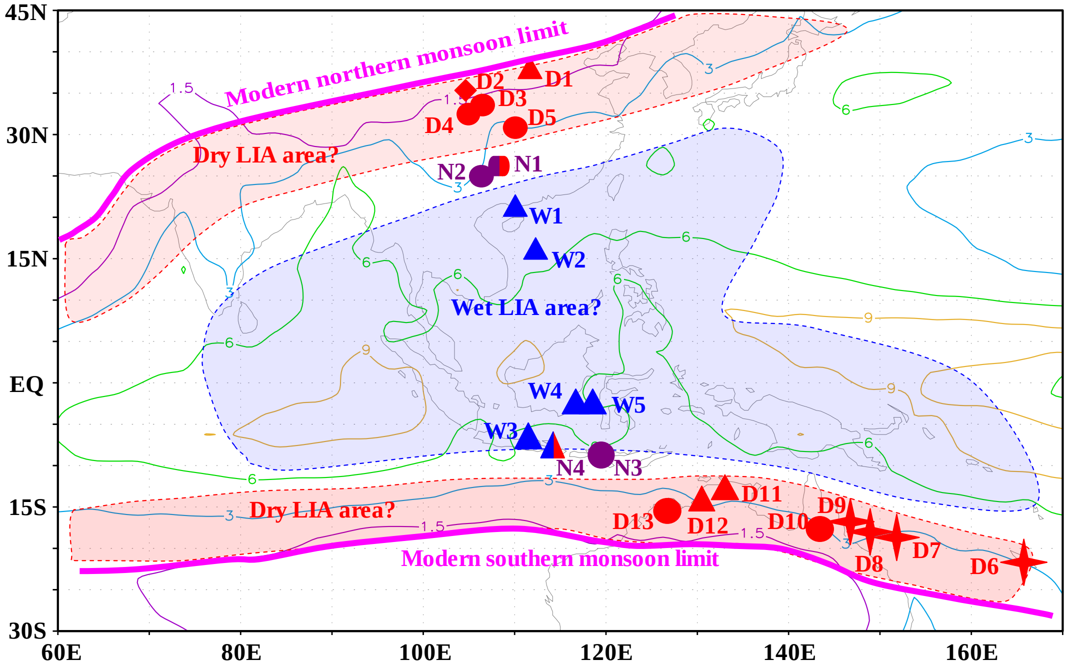

Figure s7: Schematic map depicting the current extent of the monsoon/ITCZ in the East Asia-Australia area, and the hypothesized contraction of the monsoon/ITCZ zone during the LIA. The hydrologic records in Figure 1 and 2 are also marked here. The pink lines indicate the northern and southern limits of modern EASM and ASM. The red shaded areas indicate the areas with possibly lower precipitation during the LIA than during the MCA. The blue shaded area indicates the area with possibly more precipitation during the LIA than occurred during the MCA. The monsoon/ITCZ rainbelt would spend more time in the blue shaded area during the LIA than it did during the previous MCA, while the rainbelt would spend less time in, or even disappear from, the red shaded areas during the LIA.

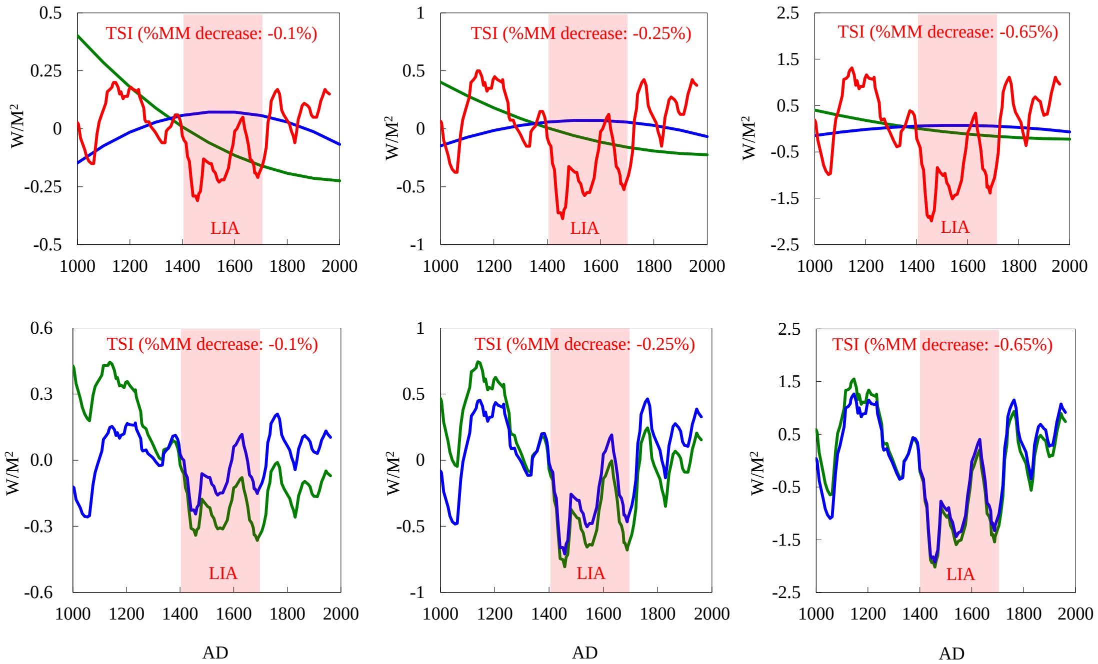

Figure s8: Top panels show the solar forcing variations over the last millennium caused by the changes of the total solar irradiance (TSI, red line)[1] and orbital parameters (green is the July insolation at 23.5ºN and blue is the January insolation at 23.5ºS)[55]. The TSI curve in the left, middle and right panel has been calculated by assuming a TSI reduction by -0.1%, -0.25 % and -0.65% during the Maunder Minimum[1,56,57]. Please note the drastically different amplitude of solar forcing as indicated by the changing vertical scales for each TSI scenario and that the January and July dates may have been be shifted by about 17 days from AD 1000 to 2000 owing to apsidal precession[58] of the Earth-Sun orbits. The bottom panel shows the total solar forcing of the Northern Hemisphere at 23.5ºN (green) and the Southern Hemisphere at 23.5ºS (blue), calculated by adding up the solar forcing that results from changes in the intrinsic solar output and orbital parameters. The total solar forcing for the last 1000 years shows the dominance of the symmetric solar forcing rooted in the intrinsic solar magnetic activity variations rather than the anti-symmetric solar insolation forcing caused by the Sun-Earth orbital precession parameters.

It should be noted that the range of the TSI amplitude change of about 0.2% to 0.6% shown in Bard et al (2000)[1] is fully consistent with the empirical results shown in Zhang et al. (1994)[59], and that the independent estimates for TSI variations from the study of solar-type stars by Zhang et al. (1994) has not yet been objectively ruled out. We also wish to emphasize that our adopted choice of TSI amplitude of variations follow empirically constrained results based on observations rather than theoretical modeling works. That fact explains why the TSI in our climate simulation experiments (-0.25%) and Liu et al (2009) (-0.3%) are still relatively larger than the -0.1% recommended by Schmidt et al. (2011) for TSI change between the Maunder Minimum and present[57]. The 0.1% value is roughly rooted in the measured TSI peak-to-peak amplitude for the 11-yr solar cycle variations (see e.g., Willson and Hudson 1991)[60], whereas a drastically smaller TSI amplitude value of 0.04% listed in Schmidt et al (2011) is specifically related to the theoretical assumption of no (or only very small) TSI change in the published work of Wang et al. (2005)[61]. Because the small TSI amplitude variation is largely a theoretical assumption rather than any confirmed, measured reality, we have chosen to adopt -0.25% as the optimal TSI amplitude value for our climate simulation experiments shown in Figure 3d and Figure s9.

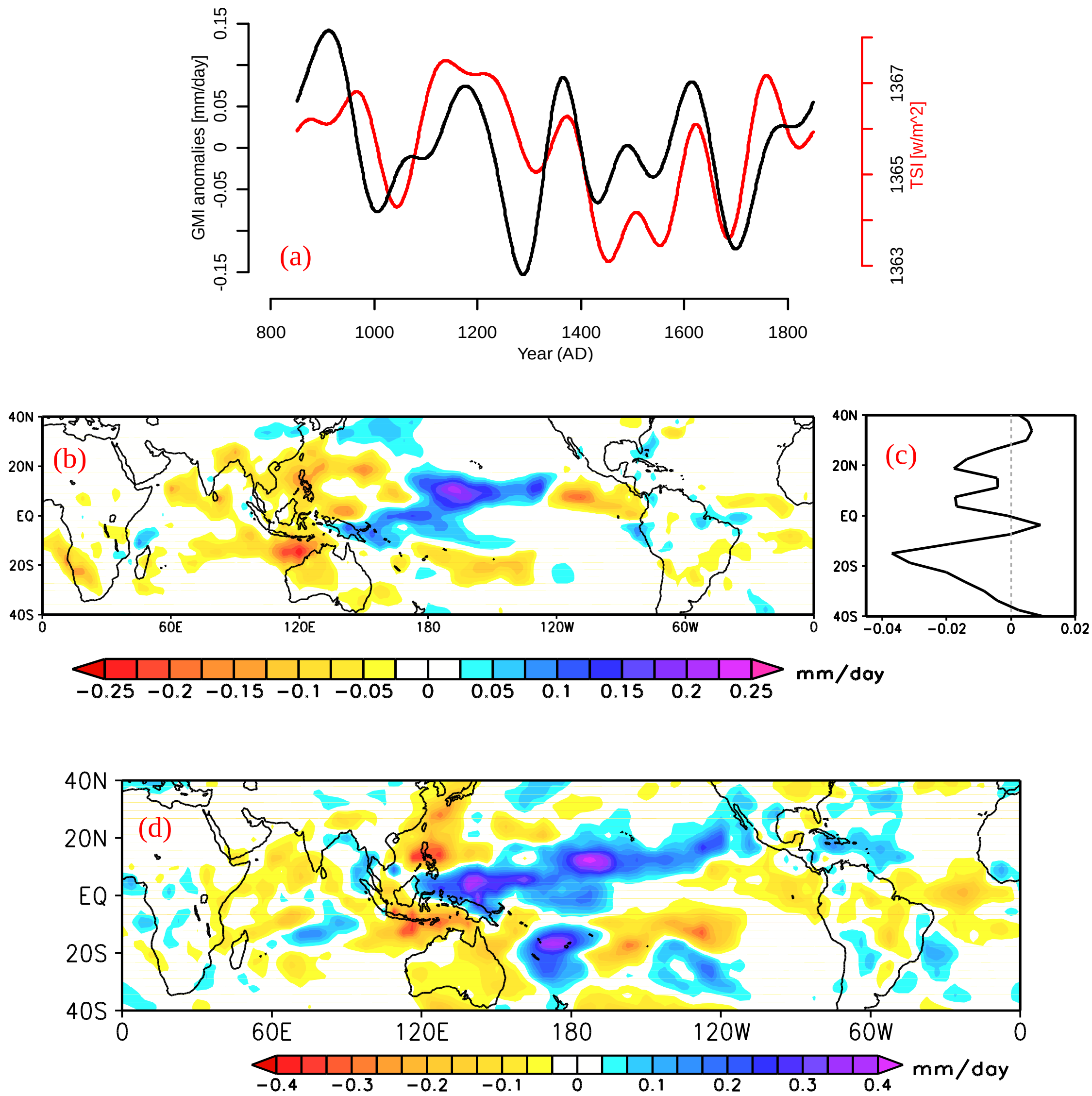

Figure s9: (a) Low-pass (> 90-year timescales) filtered global monsoon index (GMI; black) based on MIP-ESM last millennium simulation with only TSI (red) as external forcing[37]. In this simulation, 0.25% TSI change from the Maunder Minimum to present has been applied (see Fig. s8 for our choice of the TSI data and amplitude). Here the GMI is defined as the sum of local summer precipitation over the monsoon domains in both hemispheres, where the annual range (MJJAS precipitation minus NDJFM precipitation in the NH and NDJFM minus MJJAS precipitation in the SH) of precipitation exceeds 2 mm/day and the local summer precipitation exceeds 55% of annual rainfall[36]. (b) Summer precipitation pattern under low solar activity conditions over the last millennium. The anomalies have been calculated by regression analysis of the GMI with the local summer (June to August in the Northern Hemisphere and December to February in the Southern Hemisphere) precipitation during AD 850-1850. A low-pass filter has been applied to both the GMI and precipitation filed prior to the analysis in order to concentrate on precipitation pattern associated with the solar variability on multidecadal-to-centennial timescales. The high correlation (r=0.45 when GMI lags TSI by 10 years) between the two indices suggests that the centennial precipitation pattern here is primarily forced by the solar variability. The zonal mean precipitation pattern, which revealed decreased monsoon precipitation in both northern and southern tropical-subtropical monsoon area, and increased rainfall in equatorial area, is also given (c). (d) The simulated annual mean precipitation anomaly during the late Maunder minimum[62] of the LIA (AD 1690-1740) with reference to the long-term (AD 1000-1800) mean (i.e., similar to Fig. 3d, but Fig. 3d focuses on western Pacific region while here a circum-global view over the tropics is presented). Here the interval for LIA has been chosen according to the simulated GMI in (a), when the model has better performance on simulating the monsoonal precipitation associated with the solar irradiance during the Maunder Minimum.

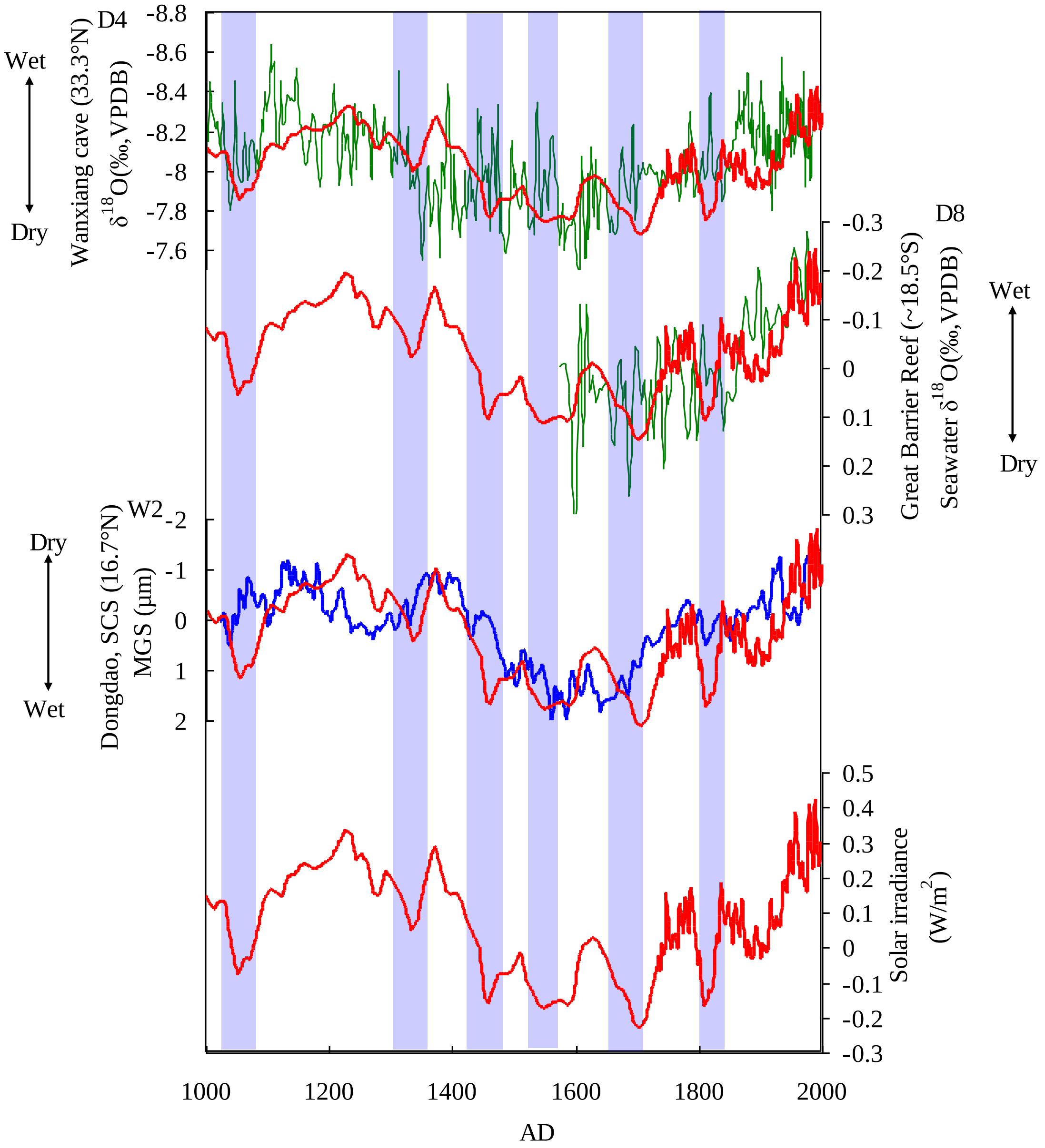

Figure s10: Comparison between solar irradiance[2] (in the original net radiative forcing units defined in Ref. 2) and hydrological records D4[3], D8[4] and W2[5] from the Asian-Australian monsoon area. The vertical shaded bars indicate time intervals of decadal-scale solar irradiance minima. Significant correlations were observed between solar irradiance and hydrological records D8 ($r = 0.54$, $p<0.05$) and W2 ($r = 0.68$, $p<0.05$). We adopted the composite solar irradiance record from Ref. 2, which is the splice of the 0.25% TSI series from Ref. 1 for 1000-1610 AD (hence similar to results shown in the top panels of Fig. s8); another higher temporal resolution TSI taken from Ref. 2 was used for the 1610-1998 AD interval. It is worth noting that the calculated correlations between proxy records and solar activity record are dominated by the low-frequency (i.e., centennial and bicentennial) variability, not the decadal variability. Moreover, only parts of (not all) decadal variability in proxy records are correlated with the solar activity record. Some reasons exist that could explain the disagreement between the decadal variation of proxy records and solar activity records, including time delays for hydrologic changes in response to solar activity forcing, spatial differences of the local and regional rainfalls in response to solar variations (e.g., wet, dry and no changes in different regions in response to the same solar minima) and the quality of the proxy records (e.g., time resolution, error of age model).

Supplementary Table

Table s1: RWI values and t-test statistics calculated for the difference of two means (LIA vs. MCA or Recent 150 years) for the EASM-ASM hydrologic records in Fig. 1 and Fig.2. In addition, we have also performed sensitivity tests to confirm the robustness of our adopted RWI results but choosing slightly different start and end intervals for MCA, LIA and current warm period (e.g., LIA covering AD 1400-1850 instead of the main choice of AD 1400-1700 adopted or MCA to be from AD 1000-1400 compared to the chosen MCA interval of AD 1000-1300). We did not find any drastic change to our RWI and t-test results under such perturbations. Only some slight changes were observed in the records from transition area, such as N1, N3 et al.

Region	Record Number	Reference	RWI, p value of the t-test (two tails), Hydrological condition	
			Hydrological condition between LIA and MCA	Hydrological condition between LIA and recent 150 years
EASM	D1	[39]	-85%, p<0.01, Dry	-153%, p<0.01, Dry
EASM	D2	[40]	-110%, p<0.01, Dry	-74%, p<0.01, Dry
EASM	D3	[8]	-112%, p<0.01, Dry	-102%, p<0.01, Dry
EASM	D4	[3]	-145%, p<0.01, Dry	-144%, p<0.01, Dry
EASM	D5	[7]	-96%, p<0.01, Dry	-90%, p<0.01, Dry
EASM	N1	[9]	-24%, p>0.05, No apparent change	-153%, p<0.01, Dry
EASM	N2	[41]	29%, p>0.05, No apparent change	24%, p>0.05*, No apparent change
EASM	W1	[42,43]	121%, p<0.01, Wet	189%, p<0.01, Wet
EASM	W2	[5,27]	156%, p<0.01, Wet	163%, p<0.01, Wet
ASM	D6	[47-49]		-71%, p<0.01, Dry
ASM	D7	[50]		-62%, p<0.05 (0.021), Dry
ASM	D8	[4]		-143%, p<0.01, Dry
ASM	D9	[51]		-92%, p<0.01, Dry
ASM	D10	[44,45]	-92%, p<0.01, Dry	-80%, p<0.01, Dry
ASM	D12	[10]	-155%, p<0.01, Dry	-178%, p<0.01, Dry
ASM	D13	[46]	-105%, p<0.01, Dry	-142%, p<0.01, Dry
ASM	N3	[52]	87%, p>0.05, No apparent change	41%, p>0.05, No apparent change
ASM	N4	[53]	78%, p<0.01, Wet	-138%, p<0.01, Dry
ASM	W3	[54]	124%, p<0.01, Wet	176%, p<0.01, Wet
ASM	W4	[18]	152%, p<0.01, Wet	142%, p<0.05 (=0.023), Wet
ASM	W5	[19,21]	173%, p<0.01, Wet	86%, p<0.01, Wet

References:

1 Bard, E., Raisbeck, G., Yiou, F. & Jouzel, J. Solar irradiance during the last 1200 years based on cosmogenic nuclides. *Tellus B* **52**, 985-992 (2000).

2 Crowley, T. J. Causes of climate change over the past 1000 years. *Science* **289**, 270-277 (2000).

3 Zhang, P. Z. *et al.* A Test of Climate, Sun, and Culture Relationships from an 1810-Year Chinese Cave Record. *Science* **322**, 940-942 (2008).

4 Hendy, E. *et al.* Abrupt decrease in tropical Pacific sea surface salinity at end of Little Ice Age. *Science* **295**, 1511-1514 (2002).

5 Yan, H. *et al.* South China Sea hydrological changes and Pacific Walker Circulation variations over the last millennium. *Nature Communications* **2**, 293 (2011).

6 Steinke, S. *et al.* Mid to Late-Holocene Australian-Indonesian summer monsoon variability. *Quaternary Science Reviews* **93**, 142-154 (2014).

7 Hu, C. *et al.* Quantification of Holocene Asian monsoon rainfall from spatially separated cave records. *Earth and Planetary Science Letters* **266**, 221-232 (2008).

8 Tan, L. *et al.* Centennial-to decadal-scale monsoon precipitation variability in the semi-humid region, northern China during the last 1860 years: Records from stalagmites in Huangye Cave. *The Holocene* **21**, 287-296 (2010).

9 Wang, Y. J. *et al.* The Holocene Asian monsoon: Links to solar changes and North Atlantic climate. *Science* **308**, 854-857 (2005).

10 Wasson, R., Bayliss, P. & Clelland, S. River flow and climate in the 'top end' of Australia for the last 1000 years, and the Asian-Australian monsoon. In Kakadu National Park Landscape Symposia Series 2007-2009. Symposium 4: Climate change. ed S Winderlich, 6-7 August 2008, Gagudju Crocodile Holiday Inn Kakadu National Park. Internal Report 567, January, Supervisiong Scientist, Darwin, 15-31. (2010).

11 Verschuren, D., Laird, K. R. & Cumming, B. F. Rainfall and drought in equatorial east Africa during the past 1,100 years. *Nature* **403**, 410-414 (2000).

12 Garcin, Y. *et al.* Solar and anthropogenic imprints on Lake Masoko (southern Tanzania) during the last 500 years. *Journal of Paleolimnology* **37**, 475-490 (2007).

13 Hodell, D. A., Brenner, M., Curtis, J. H. & Guilderson, T. Solar forcing of drought frequency in the Maya lowlands. *Science* **292**, 1367-1370 (2001).

14 Poore, R., Quinn, T. & Verardo, S. Century-scale movement of the Atlantic Intertropical Convergence Zone linked to solar variability. *Geophysical Research Letters* **31**, L12214 (2004).

15 Black, D. E., Thunell, R. C., Kaplan, A., Peterson, L. C. & Tappa, E. J. A 2000-year record of Caribbean and tropical North Atlantic hydrographic variability. *Paleoceanography* **19**, PA2022 (2004).

16 Burn, M. J. & Palmer, S. E. Solar forcing of Caribbean drought events during the last millennium. *Journal of Quaternary Science* **29**, 827-836 (2013).

17 Stríkis, N. M. *et al.* Abrupt variations in South American monsoon rainfall during the Holocene based on a speleothem record from central-eastern Brazil. *Geology* **39**, 1075-1078 (2011).

18 Tierney, J., Oppo, D., Rosenthal, Y., Russell, J. & Linsley, B. Coordinated hydrological regimes in the Indo-Pacific region during the past two millennia. *Paleoceanography* **25**,

PA1102 (2010).

19 Oppo, D. W., Rosenthal, Y. & Linsley, B. K. 2,000-year-long temperature and hydrology reconstructions from the Indo-Pacific warm pool. *Nature* **460**, 1113-1116 (2009).

20 Yan, H. *et al.* A record of the Southern Oscillation Index for the past 2,000 years from precipitation proxies. *Nature Geoscience* **4**, 611-614 (2011).

21 Newton, A., Thunell, R. & Stott, L. Climate and hydrographic variability in the Indo-Pacific Warm Pool during the last millennium. *Geophysical Research Letters* **33**, L19710 (2006).

22 Conroy, J. L. *et al.* Unprecedented recent warming of surface temperatures in the eastern tropical Pacific Ocean. *Nature Geoscience* **2**, 46-50 (2009).

23 Kennett, D. J. & Kennett, J. P. Competitive and cooperative responses to climatic instability in coastal southern California. *American Antiquity* **65**, 379-395 (2000).

24 Cobb, K. M., Charles, C. D., Cheng, H. & Edwards, R. L. El Nino/Southern Oscillation and tropical Pacific climate during the last millennium. *Nature* **424**, 271-276 (2003).

25 Conroy, J. L., Overpeck, J. T. & Cole, J. E. El Nino/Southern Oscillation and changes in the zonal gradient of tropical Pacific sea surface temperature over the last 1.2 ka. *PAGES news* **18**, 32-34 (2010).

26 Graham, N. E. *et al.* Tropical Pacific - mid-latitude teleconnections in medieval times. *Climatic Change* **83**, 241-285 (2007).

27 Liu, X. D. *et al.* A 1,100-year palaeoenvironmental record inferred from stable isotope and trace element compositions of ostracode and plant caryopses in sediments of Cattle Pond, Dongdao Island, South China Sea. *Journal of Paleolimnology* **40**, 987-1002 (2008).

28 Sachs, J. P. *et al.* Southward movement of the Pacific intertropical convergence zone AD 1400-1850. *Nature Geoscience* **2**, 519-525 (2009).

29 Conroy, J. L., Overpeck, J. T., Cole, J. E., Shanahan, T. M. & Steinitz-Kannan, M. Holocene changes in eastern tropical Pacific climate inferred from a Galapagos lake sediment record. *Quaternary Science Reviews* **27**, 1166-1180 (2008).

30 Moy, C. M., Seltzer, G. O., Rodbell, D. T. & Anderson, D. M. Variability of El Nino/Southern Oscillation activity at millennial timescales during the Holocene epoch. *Nature* **420**, 162-165 (2002).

31 Mann, M., Cane, M., Zebiak, S. & Clement, A. Volcanic and solar forcing of the tropical Pacific over the past 1000 years. *Journal of Climate* **18**, 447-456 (2005).

32 Clement, A. C., Seager, R., Cane, M. A. & Zebiak, S. E. An ocean dynamical thermostat. *Journal of Climate* **9**, 2190-2196 (1996).

33 Zebiak, S. & Cane, M. A Model El Ni –Southern Oscillation. *Monthly Weather Review* **115**, 2262-2278 (1987).

34 Vecchi, G. A. *et al.* Weakening of tropical Pacific atmospheric circulation due to anthropogenic forcing. *Nature* **441**, 73-76 (2006).

35 Held, I. & Soden, B. Robust responses of the hydrological cycle to global warming. *Journal of Climate* **19**, 5686-5699 (2006).

36 Liu, J. *et al.* Centennial variations of the global monsoon precipitation in the last millennium: Results from ECHO-G model. *Journal of Climate* **22**, 2356-2371 (2009).

37 Jungclaus, J. H. *et al.* Climate and carbon-cycle variability over the last millennium. *Climate of the Past* **6**, 723-737 (2010).

38 Man, W. M., Zhou, T. J. & Jungclaus, J. H. Simulation of the East Asian Summer Monsoon

during the Last Millennium with the MPI Earth System Model. *Journal of Climate* **25**, 7852-7866, doi:Doi 10.1175/Jcli-D-11-00462.1 (2012).

39 Liu, J. B. *et al.* Humid medieval warm period recorded by magnetic characteristics of sediments from Gonghai Lake, Shanxi, North China. *Chinese Science Bulletin* **56**, 2464-2474 (2011).

40 Tan, L. C., Cai, Y. J., Yi, L., An, Z. S. & Ai, L. Precipitation variations of Longxi, northeast margin of Tibetan Plateau since AD 960 and their relationship with solar activity. *Climate of the Past* **4**, 19-28 (2008).

41 Qin, J. *et al.* High resolution stalagmite record of climate change since 800a A.D. in Libo, Guizhou. *Carsologica Sinica (In Chinese with English abstract)* **27**, 266-272 (2008).

42 Chu, G. *et al.* The ‘mediaeval warm period’drought recorded in Lake Huguangyan, tropical South China. *The Holocene* **12**, 511-516 (2002).

43 Zeng, Y. *et al.* The wet little Ice age recorded by sediments in Huguangyan Lake, tropical South China. *Quaternary International* **263**, 55-62 (2011).

44 Burrows, M., Fenner, J. & Haberle, S. Testing peat humification analysis in an Australian context: identifying wet shifts in regional climate over the past 4000 years. *Mires and Peat* **14**, 1-19 (2014).

45 Burrows, M. A., Fenner, J. & Haberle, S. G. Humification in northeast Australia: Dating millennial and centennial scale climate variability in the late Holocene. *The Holocene* **24**, 1707-1718 (2014).

46 Denniston, R. F. *et al.* A Stalagmite record of Holocene Indonesian-Australian summer monsoon variability from the Australian tropics. *Quaternary Science Reviews* **78**, 155-168 (2013).

47 DeLong, K. L., Quinn, T. M., Taylor, F. W., Shen, C.-C. & Lin, K. Improving coral-base paleoclimate reconstructions by replicating 350 years of coral Sr/Ca variations. *Palaeogeography, Palaeoclimatology, Palaeoecology* **373**, 6-24 (2013).

48 Quinn, T. M. *et al.* A multicentury stable isotope record from a New Caledonia coral: Interannual and decadal sea surface temperature variability in the southwest Pacific since 1657 AD. *Paleoceanography* **13**, 412 (1998).

49 Stephans, C. L., Quinn, T. M., Taylor, F. W. & Corrège, T. Assessing the reproducibility of coral-based climate records. *Geophysical Research Letters* **31** (2004).

50 Calvo, E. *et al.* Interdecadal climate variability in the Coral Sea since 1708 AD. *Palaeogeography, Palaeoclimatology, Palaeoecology* **248**, 190-201 (2007).

51 Lough, J. M. Great Barrier Reef coral luminescence reveals rainfall variability over northeastern Australia since the 17th century. *Paleoceanography* **26**, PA2201 (2011).

52 Griffiths, M. *et al.* Increasing Australian-Indonesian monsoon rainfall linked to early Holocene sea-level rise. *Nature Geoscience* **2**, 636-639 (2009).

53 Konecky, B. L. *et al.* Intensification of southwestern Indonesian rainfall over the past millennium. *Geophysical Research Letters* **40**, 386-391 (2013).

54 Rodysill, J. R. *et al.* A paleolimnological record of rainfall and drought from East Java, Indonesia during the last 1,400 years. *Journal of Paleolimnology* **47**, 1-15 (2012).

55 Laskar, J., Fienga, A., Gastineau, M. & Manche, H. La2010: a new orbital solution for the long-term motion of the Earth. *Astronomy & Astrophysics* **532**, A89 (2011).

56 Steinhilber, F. *et al.* 9,400 years of cosmic radiation and solar activity from ice cores and tree

rings. *Proceedings of the Natational Academy of Sciences (USA)* **109**, 5967-5971 (2012).

57 Schmidt, G. A. *et al.* Climate forcing reconstructions for use in PMIP simulations of the last millennium (v1.0). *Geoscientific Model Development* **4**, 33-45 (2011).

58 Steel, D. Perihelion precession, polar ice and global warming. *Journal of Cosmology* **22**, 10106-10129 (2013).

59 Zhang, Q. *et al.* A method of determining possible brightness variations of the Sun in past centuries from observations of solar-type stars. *The Astrophysical Journal* **427**, L111-L114 (1994).

60 Willson, R. C. & Hudson, H. S. The Suns Luminosity over a Complete Solar-Cycle. *Nature* **351**, 42-44 (1991).

61 Wang, Y. M., Lean, J. L. & Sheeley, N. R. Modeling the sun's magnetic field and irradiance since 1713. *The Astrophysical Journal* **625**, 522-538 (2005).

62 Vaquero, J. M. & Trigo, R. M. Redefining the limit dates for the Maunder Minimum. *New Astronomy* **34**, 120-122, (2015).